

A new sample of giant radio galaxies from the WENSS survey

I. Sample definition, selection effects and first results^{*,**}

A. P. Schoenmakers^{1,2,3,***}, A. G. de Bruyn^{3,4}, H. J. A. Röttgering², and H. van der Laan¹

¹ Astronomical Institute, Utrecht University, PO Box 80000, 3508 TA Utrecht, The Netherlands

² Sterrewacht Leiden, Leiden University, PO Box 9513, 2300 RA Leiden, The Netherlands

³ ASTRON, PO Box 2, 7990 AA Dwingeloo, The Netherlands

⁴ Kapteyn Astronomical Institute, University of Groningen, PO Box 800, 9700 AV Groningen, The Netherlands

Received 22 August 2000 / Accepted 23 May 2001

Abstract. We have used the Westerbork Northern Sky Survey (WENSS) to define a sample of 47 low redshift ($z \lesssim 0.4$) giant radio galaxies. This is the largest sample yet of such radio sources originating from a single survey. We present radio maps of the newly discovered giants and optical images and spectra of their host galaxies. We present some of their properties and discuss the selection effects. We investigate the distribution of the sources in the radio power – linear size P – D diagram, and how these parameters relate to the redshifts of the sources in our sample. We find a strong drop in the number of sources with a linear size above 2 Mpc. We argue that this is not a result of selection effects, but that it indicates either a strong luminosity evolution of radio sources of such a size, or that a large fraction of radio sources “switch off” before they are able to grow to a size of 2 Mpc.

Key words. galaxies: active – intergalactic medium – galaxies: jets – radio continuum: galaxies

1. Introduction

The central activity in a fraction of Active Galactic Nuclei (AGN) is capable of producing relativistic outflows of matter, the so-called “jets”, for a prolonged period of time, possibly up to a few 10^8 yr. These jets, when powerful enough, inflate a cocoon (e.g. Scheuer 1974; Falle 1991) which expands first in the Interstellar Medium (ISM) and later in the Intergalactic Medium (IGM) of the host galaxy. The evolution of such cocoons is traced by the radio lobes, which in themselves are only a (albeit important) “side effect” caused by the presence of magnetic fields in the cocoon.

The giant radio galaxies (GRGs) are those radio sources whose lobes span a (projected) distance of above 1 Mpc¹. As such, GRGs must represent a late phase in the evolution of radio sources. Models of radio source evolu-

tion (e.g. Kaiser et al. 1997; Blundell et al. 1999) predict the radio power and linear size evolution of powerful radio sources with time. According to these models, GRGs must be extremely old (i.e. typically older than 10^8 yr) and probably also located in underdense environments, as compared to smaller radio sources of comparable radio power (e.g. Kaiser & Alexander 1999).

Multi-frequency radio observations (Mack et al. 1998) have shown that spectral ages of GRGs are of the same order as expected from source evolution models. It is, however, not clear at all whether *spectral* ages are representative of the *dynamical* ages (e.g. Parma et al. 1999). This questions the validity of radio-based determinations of the properties of the environments of these sources. Still, constraints on the environments of GRGs are of high importance since the radio lobes of these sources penetrate deeply into the intergalactic medium. It is almost impossible to find the properties of this medium, otherwise than from studies of such radio lobes (e.g. Subrahmanyam & Saripalli 1993).

A major problem for such studies is that currently known GRGs have not been uniformly selected. The difficulties encountered while selecting extended radio sources have been demonstrated by Saunders et al. (1987), who have searched for GRGs in a small region of the 151-MHz 6C survey. The 6C survey, with only 30 mJy beam⁻¹ RMS-noise and a beamsize of $4.2' \times 4.2'$ cosec δ FWHM (with δ the declination) has an excellent sensitivity to large,

Send offprint requests to: A. P. Schoenmakers,
e-mail: Schoenmakers@astron.nl

* The catalogue is only available in electronic form at the CDS via anonymous ftp to cdsarc.u-strasbg.fr (130.79.128.5) or via

<http://cdsweb.u-strasbg.fr/cgi-bin/qcat?J/A+A/374/861>

** The Appendix is only available in electronic form at <http://www.edpsciences.org>

*** Present address: ASTRON, PO Box 2, 7990 AA Dwingeloo, The Netherlands.

¹ We use $H_0 = 50 \text{ km s}^{-1} \text{ Mpc}^{-1}$ and $q_0 = 0.5$ throughout this paper.

faint objects. However, using higher resolution observations they found that only at integrated flux densities above 5 Jy has a radio source larger than $5'$ a good chance of being a genuine GRG in the 6C. At a flux density level of 1 Jy, Saunders et al. find that most of the sources which appear as large extended structures on the 6C survey maps are the result of confusion of physically unrelated sources. Their work demonstrates that 1) an efficient search for GRGs has to be done with sufficient angular resolution to minimize confusion problems and that 2) it should be done with a high sensitivity, also for large-scale structures (up to a few tens of arcmin) on the sky. The recently completed WENSS survey (Rengelink et al. 1997) meets both these demands.

In this paper we report of the selection of new giant radio sources from the WENSS. Subsequent papers will present additional radio observations (Schoenmakers et al. 2000b), a more detailed analysis of the spectroscopic data and a discussion of the evolution of GRGs (in preparation, but see Schoenmakers 1999a). In Sect. 2 we outline the selection technique and criteria. Section 2.5 presents the strategy we have adopted for finding the optical identifications, and Sect. 3 describes the spectroscopic observations of these identifications. In Sect. 4 we present the first results of the new sample of GRGs: Flux densities, linear sizes, redshifts, etc. A discussion of these results and on the sensitivity of the WENSS survey to extended radio sources is given in Sect. 5.

Throughout this paper, a spectral index α is defined according to the relation $S_\nu \propto \nu^\alpha$ between flux density S_ν at frequency ν , and the frequency ν .

2. Sample selection

2.1. The WENSS survey

The Westerbork Northern Sky Survey is a 325-MHz survey of the sky above $+28^\circ$ declination. About a quarter of this area has also been observed at a frequency of 609 MHz. The unique aspect of WENSS is that it is sensitive to spatial structures over 1 degree on the sky at 325 MHz. The limiting flux density to unresolved sources is about 15 mJy (5σ) and the *FWHM* of the beam is $54'' \times 54'' \cos \delta$, with δ the declination. A detailed description of the observing and data reduction techniques used can be found in Rengelink et al. (1997). The sky area above $+74^\circ$ declination has been observed with an increased total bandwidth, so that the limiting flux density to unresolved sources is about 10 mJy (5σ) in this sky area.

Using the Wieringa (1991) source counts at 325-MHz, the flux density at which the same amount of confusion in the WENSS as Saunders et al. (1987) encountered in the 6C survey can be calculated. For a typical radio source spectral index of -0.8 , a similar amount of confusion can be expected in the WENSS at a flux density of ~ 400 mJy, which is almost seven times lower than that for the 6C survey. Similarly, it can be shown that confusion would

dominate the selection sources only below 20 mJy in the WENSS survey, which is below its completeness limit of ~ 30 mJy (Rengelink et al. 1997). This implies that we should be able to efficiently find GRGs in the WENSS down to relatively low flux density levels.

2.2. Selection criteria

In order for a source to be a candidate low redshift GRG, we have used the following criteria. A candidate GRG must have:

1. an angular size larger than 5 arcminute, and
2. a distance to the galactic plane of more than 12.5 degree.

The angular size lower limit of $5'$ is the size at which some basic morphological information of a source can still be obtained at all declinations the survey has covered. this corresponds to a physical size of ~ 750 kpc at $z = 0.1$, ~ 1300 kpc at $z = 0.2$ and ~ 1700 kpc at $z = 0.3$, and will therefore introduce a redshift-dependent linear size bias in the sample. To avoid high galactic extinction values and confusion by a large surface density of foreground stars, we have restricted ourselves to galactic latitudes above 12.5° . This results in a survey area of ~ 2.458 steradian ($\sim 8100^\square$).

Table 1 presents all previously discovered GRGs whose angular size and position on the sky agree with the above selection criteria. The majority of these are smaller than 2 Mpc in size. If their sizes are characteristic for the whole population of GRGs, we thus expect that the majority of selected sources will have a redshift below ~ 0.35 . Assuming that the host galaxies are not less luminous than those of the LRL sample of powerful radio sources (Laing et al. 1983) they should be identifiable on the Digitized POSS-I survey (DSS).

2.3. Selection method

Candidate radio sources were selected using a visual inspection of the WENSS radio maps. We preferred this method over possibly more objective, machine controlled selection methods because the complexity of the WENSS radio maps (i.e. the high source surface density and the unavoidable presence of spurious artefacts such as low-level sidelobes of bright sources, etc.) and the wide variety in possible morphologies would make it very difficult to tune such an algorithm. Looking at the maps allows one to easily recognize low-level extended structures in a crowded field.

Above declination $+74^\circ$ we have initially selected our candidates using the earlier available NVSS survey maps (Condon et al. 1998), but we subsequently repeated the selection using the WENSS maps. We found that no WENSS selected candidates were omitted using the NVSS. On the contrary, we have identified two NVSS sources (B 1044+745 and B 0935+743) that we most likely

Table 1. List of all previously known GRGs (i.e. before 1998) in the area of the sky covered by the WENSS and fulfilling our selection criteria. Column 1 gives the name of the source in IAU-format; Col. 2 gives the more common name of the source, if available; Cols. 3 and 4 give the coordinates of the host galaxy in B1950.0; Cols. 5 and 6 give the redshift of the host galaxy and a reference to it; Col. 7 gives the projected linear size of the radio source in Mpc; Col. 8 designate the morphological type of the radio source, i.e. FRI or FR II or an intermediate type, FRI/II. If a “B” is added, it means that the host galaxy is a broad-line object, a “Q” means that it is a quasar. Column 9 gives a reference to radio maps in which the radio morphology can be studied. Columns 10 and 11 give the flux density at 325 MHz and the reference for this value.

(1)	(2)	(3)	(4)	(5)	(6)	(7)	(8)	(9)	(10)	(11)
IAU Name	Other name	RA	Dec	z	Refs.	Size	Type	Refs.	S_{325}	Refs.
		(B1950.0)				[Mpc]	FR		[Jy]	
B 0050+402		00 50 45.1	40 11 10.0	0.1488	DJ95	1.5	II	V89	1.41 ± 0.04	WE
B 0055+300	NGC 315	00 55 05.6	30 04 56.8	0.0167	C75	1.7	I/II	W81	9.71 ± 0.18	M97
B 0104+321	3C 31	01 04 39.2	32 08 44.0	0.0169	S97	1.3	I	S83	13.67 ± 0.28	WE
B 0109+492	3C 35	01 09 04.1	49 12 40.1	0.06701	B72	1.1	II	B82	7.19 ± 0.15	WE
B 0136+396	4C 39.04	01 36 33.6	39 41 51.2	0.2107	S73	1.6	II	FB78,H79	4.75 ± 0.10	WE
B 0157+405	4C 40.09	01 57 22.4	40 34 34.2	0.0827	DJ95	1.9	I/II	V89	2.98 ± 0.08	WE
B 0309+411		03 09 44.8	41 08 48.7	0.134	B89	1.8	II-B	B89	1.38 ± 0.04	WE
B 0745+560	DA 240	07 45 46.1	56 01 56.2	0.0356	W74	2.0	II	S81	17.05 ± 0.35	M97
B 0821+695		08 21 01.9	69 30 25.8	0.538	L93	3.0	II	L93	0.63 ± 0.02	WE
B 0945+734	4C 73.08	09 45 09.9	73 28 22.2	0.0581	D70	1.5	II	J86	10.43 ± 0.21	WE
B 1003+351	3C 236	10 03 05.4	35 08 48.0	0.0989	S85	5.7	II	S80	13.13 ± 0.26	M97
B 1029+570	HB 13	10 29 48.2	57 00 45.8	0.045	S96	2.6	I	MA79	1.09 ± 0.04	WE
B 1209+745	4CT 74.17	12 09 36.0	74 35 45.5	0.107	M79	1.2	II	B81	2.06 ± 0.05	WE
B 1309+412		13 09 27.1	41 14 53.5	0.1103	D90	1.0	II	V89	1.61 ± 0.04	WE
B 1312+698	DA 340	13 12 22.1	69 53 10.0	0.1060	S87	1.3	II	S87	4.16 ± 0.09	WE
B 1358+305		13 58 29.3	30 33 47.7	0.206	P96	2.6	II	P96	1.84 ± 0.04	P96
B 1626+518		16 26 48.5	51 53 05.0	0.0547	G92	1.6	II-B	R96	1.62 ± 0.03	WE
B 1637+826	NGC 6251	16 37 57.0	82 38 18.6	0.023	W77	3.0	I/II	P84	11.55 ± 0.23	M97
B 2043+749	4C 74.26	20 43 13.0	74 57 08.7	0.104	R88	1.6	II-Q	R88	4.76 ± 0.10	WE

References: B72: Burbidge & Strittmattar (1972); B81: van Breugel & Willis (1981); B82: van Breugel & Jägers (1982); B89: de Bruyn (1989); C75: Colla et al. (1975); D70: Demoulin (1970); D90: Djorgovski et al. (1990); DJ95: Djorgovski et al. (1995); FB78: Fomalont & Bridle (1978); G92: de Grijp et al. (1992); H79: Hine (1979); J86: Jägers (1986); M79: Miley & Osterbrock (1979); MA79: Masson (1979); M96: Marcha et al. (1996); M97: Mack et al. (1997); P84: Perley et al. (1984); P96: Parma et al. (1996); R88: Riley et al. (1988); R96: Röttgering et al. (1996); S73: Sargent (1973); S80: Strom & Willis (1980); S81: Strom et al. (1981); S82: Saunders (1982); S83: Strom et al. (1983); S85: Spinrad et al. (1985); S86: Saripalli et al. (1986); S87: Saunders et al. (1987); S97: Simien & Prugniel (1997); V89: Vigotti et al. (1989); WE : WENSS (measured in the radio map); W74: Willis et al. (1974); W77: Wagett et al. (1977); W81: Willis et al. (1981).

would not have selected from the WENSS survey alone due to their faintness in the latter. We will elaborate on this when we discuss the selection effects (Sect. 5.1).

2.4. Removing confused sources

The declination dependent beam size results in an unavoidable increase of confusion with decreasing declination. Only with higher angular resolution observations can we determine whether such sources are separate unrelated radio sources. We have used the following additional sources of radio data to achieve this:

First, where available, we have used the 612-MHz WENSS maps which have twice the resolution of the

325-MHz maps. Also the 1.4-GHz NVSS survey, which does not have a declination-dependent beam size and which covers almost the entire area of the WENSS survey, is highly useful in this respect. Furthermore, we have used the much higher resolution ($5''4$ FWHM) maps from the 1.4-GHz FIRST survey (Becker et al. 1995) where available. Also the FIRST survey has mapped a large fraction of the area observed by WENSS, notably the lower declination range away from the galactic plane. Finally, for candidates in areas of the sky where the FIRST survey was not (yet) available, we obtained short 1.4-GHz WSRT observations.

A consequence of the different methods used to eliminate confused sources is that the angular size of the objects

are not well determined in all cases. There are two important factors which influence such estimates: First, for edge-brightened sources (FR-II-type) high-resolution observations would be required for an accurate measurement, but we do not have these for all such sources and even the ones we have differ in quality and resolution. Second, for FR-I type sources the angular size measured on a map depends strongly on surface-brightness sensitivity. Therefore, sources may have been accidentally removed from the sample because of wrongly estimated sizes.

2.5. Identification of the host galaxies

We have used the digitized POSS-I survey (the ‘‘Digitized Sky Survey’’, DSS) and, in a later stage, also the digitized POSS-II survey to identify the host galaxies of the selected radio sources. The magnitude limit of the red POSS-I plates is $\sim 20-20.5$; the POSS-II is somewhat more sensitive.

Adopting the Cousin *R*-band magnitude–redshift relation for the host galaxies of the radio sources in the LRL sample (Dingley 1990), we expect to be able to identify host galaxies out to $z \sim 0.5$ (note that the transmission curves of the Cousin *R*-band and the POSS-E band are much alike).

To identify the host galaxy of a radio source which extends over several arcminutes, a radio core position is often necessary. We have used the WENSS, NVSS, FIRST and our own WSRT radio observations to identify radio cores of the selected sources. For many sources we indeed find a compact central radio source coincident with an optical galaxy in the POSS-I and/or POSS-II.

We cannot rule out that for an individual source the so-found optical galaxy is an unrelated foreground galaxy, and that the actual host galaxy of the radio source is a much farther and fainter galaxy. However, for the sample as a whole, we believe this to be only a minor problem: It would make the radio sources even larger than they already are and the chance of such an occurrence is very small anyway.

For the source B 1918+516 the POSS-I plates did not show an obvious host galaxy candidate. Therefore, an optical CCD image has been made by P.N. Best using the LDSS imaging spectrograph on the 4.2-m WHT telescope on La Palma. This image (see Fig. A.28) reveals a faint galaxy, close to a relatively bright star. We believe this galaxy to be the host galaxy, due to its proximity to the radio core.

We cross-correlated the positions of the optical galaxies with the NASA Extragalactic Database (NED). In case an optical source with known redshift is found and the resulting size of the radio source is below 1 Mpc, we removed that source from our sample. We present the list of remaining (i.e. after removing sources identified as non-GRGs on basis of NED data) candidate GRG sources in Table. A.1. We provide IAU-formatted source names, approximate coordinates of the radio sources, WENSS flux densities, approximate angular sizes and whether we are

convinced this a genuine giant radio galaxy candidate on basis of its radio morphology. We remark that many of the WENSS selected sources were rejected after a look at the maps of these sources from the NVSS survey.

3. Optical spectroscopy

Optical spectra of a large fraction of possible host galaxy of the candidates have been obtained. In order to construct an as complete as possible flux-density limited sample from our candidates, we have tried to obtain spectra and redshifts for all candidate sources in Table A.1 with a 325-MHz flux density above 1 Jy^2 .

In Table A.2 we present the log of the spectroscopic observations. On the 2.5-m INT telescope on La Palma we used the IDS-235 camera with the Ag-Red collimator and the R300V grating. The camera was equipped with a $1\text{k} \times 1\text{k}$ TEK chip. This setup results in a total wavelength coverage of $\sim 3500 \text{ \AA}$ and a pixel scale of $\sim 3.2 \text{ \AA}/\text{pixel}$ in the dispersion direction and $0''.74/\text{pixel}$ in the spatial direction. Depending on the magnitude estimated redshift of the host galaxy candidate, the central wavelength of the spectrograph was set at either 5500, 6000 or 6500 \AA . The slit-width was held constant at $2''$. Only in the case of the source B 0809+454 we used a $3''$ -wide slit because of uncertainties in the optical position at the time of observation. Flat-field observations were made at the beginning of each night by using the internal Tungsten lamp. Wavelength calibration was achieved by internal arc-lamp exposures (from CU-AR and CU-NE lamps) which were taken at the beginning of each night and immediately after each object exposure. For absolute flux calibration and to correct for the wavelength-dependent sensitivity of the instrument, several spectroscopical standard stars were observed each night, using a $5''$ -wide slit.

The spectra have been reduced using the NOAO IRAF data reduction software. One dimensional spectra have been extracted using a $4''$ -wide aperture centered on the peak of the spatial profile of the identification. The resulting spectra are shown in Figs. A.1–A.29. For each object exposure the wavelength calibration has been checked against several bright sky-lines in a non background-subtracted frame.

In addition to these observations, a spectrum of the source B 1450+333 was obtained on 8 July 1997 by

² From a recent paper by Lara et al. (2001), however, it was noted that three genuine candidate sources were missed after a first selection round from WENSS (B 1838+658, B 1919+741, B 0603+612). The source B 1838+658 has a redshift of 0.23 (NED) and is as such a GRG; for B 1919+741 the redshift is 0.194 and for B 0603+612 it is 0.227 (Lara et al. 2001). Also, the source B 1855+310 was not further observed. Further, high resolution observations by Lara et al. show that some sources, whose size was estimated to be less than $5'$ on basis of the WENSS maps, actually have angular sizes $\gtrsim 5'$ and should thus be included in our candidate sample. The implication of these findings is that the earlier made claim that we have observed a complete flux-density limited sample of GRGs (Paper II, Schoenmakers et al. 2000b), must be recalled.

P.N. Best, using the 4.2-m WHT on La Palma, equipped with the ISIS spectrograph. An optical CCD image and a spectrum of the source B 1543+845 were obtained by I. M. Gioia on 4 and 5 March 1998 using the HARIS imaging spectrograph on the 2.2-m University of Hawaii Telescope on Mauna Kea, Hawaii.

Table A.5 presents the measured redshifts and the spectral features used to determine these. The optical images and spectra of the observed host galaxies are presented in Figs. A.1–A.29. For the source B 1245+676 a high-quality spectrum and the therefrom derived redshift had been published earlier by Marcha et al. (1996). We have therefore not observed the host galaxy of this radio source again. We have, however, reobserved the source B 1310+451 in order to obtain a higher quality spectrum of the host galaxy of this source.

Several other radio and optical properties of the observed candidates, and of the three sources that were found to be GRGs from available data in the NED (B 1144+352, B 1245+676 and B 1310+451) are given in Tables A.3 and A.4.

4. First results

4.1. The number of GRGs

Of the 33 candidate sources which we have been able to identify spectroscopically, only three, and possibly five have projected linear sizes below 1 Mpc. These are B 0217+367, B 1709+465 and B 1911+479. The uncertain cases are the source B 0905+352, for which we do not have a well determined redshift yet and B 1736+375 which may consist of two unrelated radio sources. Together with the 19 known GRGs in the area of the WENSS which share our selection criteria, we have so far identified 47 GRGs. This is by far the largest sample of sources with a projected linear size above 1 Mpc selected from a single survey. We also mention the existence of the large, but highly incomplete sample of GRGs which has been compiled by Ishwara-Chandra & Saikia (1999) from the literature. Although of similar size, the sample presented in this paper is better suited for statistical investigations of the radio and optical properties of GRGs since it has been selected from a single survey and in a more uniform matter.

4.2. Distribution functions of the sample

4.2.1. Flux density distribution

Figure 1a presents a histogram of the 325-MHz flux density distribution of the sample of 47 sources. The hatched bars indicate the flux density distribution of the sample of previously known GRGs. Not surprisingly, we find that all newly discovered GRGs have flux densities below 3 Jy, only; all ten GRGs with a 325-MHz flux density above this value had already been identified as such. For the area of the sky covered by WENSS, we can therefore agree with Riley (1989) who argued that no bright extended sources are missing from the LRL sample of bright radio sources ($S_{178} > 10.9$ Jy, $\text{Dec} > +10^\circ$, $|b| > 10^\circ$). Furthermore, we

have extended the range of flux densities at which low redshift GRGs are found to sub-Jy levels. The median flux density of the combined sample is 1.15 Jy, which is almost a factor of four below the median value of the sample of previously known GRGs (see Table 2).

4.2.2. Redshift distribution

The new sample of GRGs mostly contains GRGs at $z \lesssim 0.3$ (see Fig. 1b). The only exceptions are the sources 8C 0821+695 ($z = 0.538$; Lacy et al. 1993), B 0750+434 ($z = 0.347$) and B 0925+420 ($z = 0.365$). The redshift distribution peaks at $z \sim 0.1$. The decrease in the number of sources towards higher redshift is likely to be due to the lower angular size limit used in the selection of the sample. Further, only more powerful GRGs will be selected towards higher redshift, of which the space density is likely to be lower. The median redshift of the sample of new GRGs is 0.1404, which is higher than that of the old GRGs alone (0.099; see Table 2). Since the average flux density is lower this is not surprising. The median redshift of the combined sample is 0.1175.

4.2.3. Linear size distribution

No source with a (projected) linear size exceeding that of the GRG 3C 236 has been found. This source is therefore still the largest known radio galaxy in the Universe. In Fig. 1c we have plotted the (projected) linear size distribution of our sample. The median values of the linear sizes of the old and new GRGs lie close together (see Table 2). The majority of sources have linear sizes between 1 and 2 Mpc; the distribution of the combined sample falls off strongly at a linear size of 2 Mpc. This sharp decrease was not clear from the sample of “old” GRGs only, due to the small number of sources. In Sect. 5.4 we will discuss whether the observed cut-off is a result of selection effects or an intrinsic property of the population of GRGs.

4.2.4. Radio power distribution

We calculated the emitted radio power at a rest-frame frequency of 325 MHz assuming isotropic emission. Since the redshifts are low, the radio K-correction is only small. For the new GRGs the measured spectral index between 325 and 1400 MHz has been used; for the “old” GRGs a spectral index of -0.8 has been assumed if no reliable literature value could be found. The distribution of 325-MHz radio powers has been plotted in Fig. 1d. Despite the fact that a large number of GRGs has been found at flux density values well below that of the “old” sample, the distribution of the radio powers of the new sources largely overlaps that of the old sources. This is related to the, on average, higher redshifts of the new sources. The combined sample is distributed rather uniformly between 10^{25} and 10^{27} W Hz^{-1} ; the sharp peak at the radio power bin centered on $10^{26.1}$ W Hz^{-1} is most likely a result of small number statistics. At 325 MHz, the traditional separation between FR II and FR I-type sources

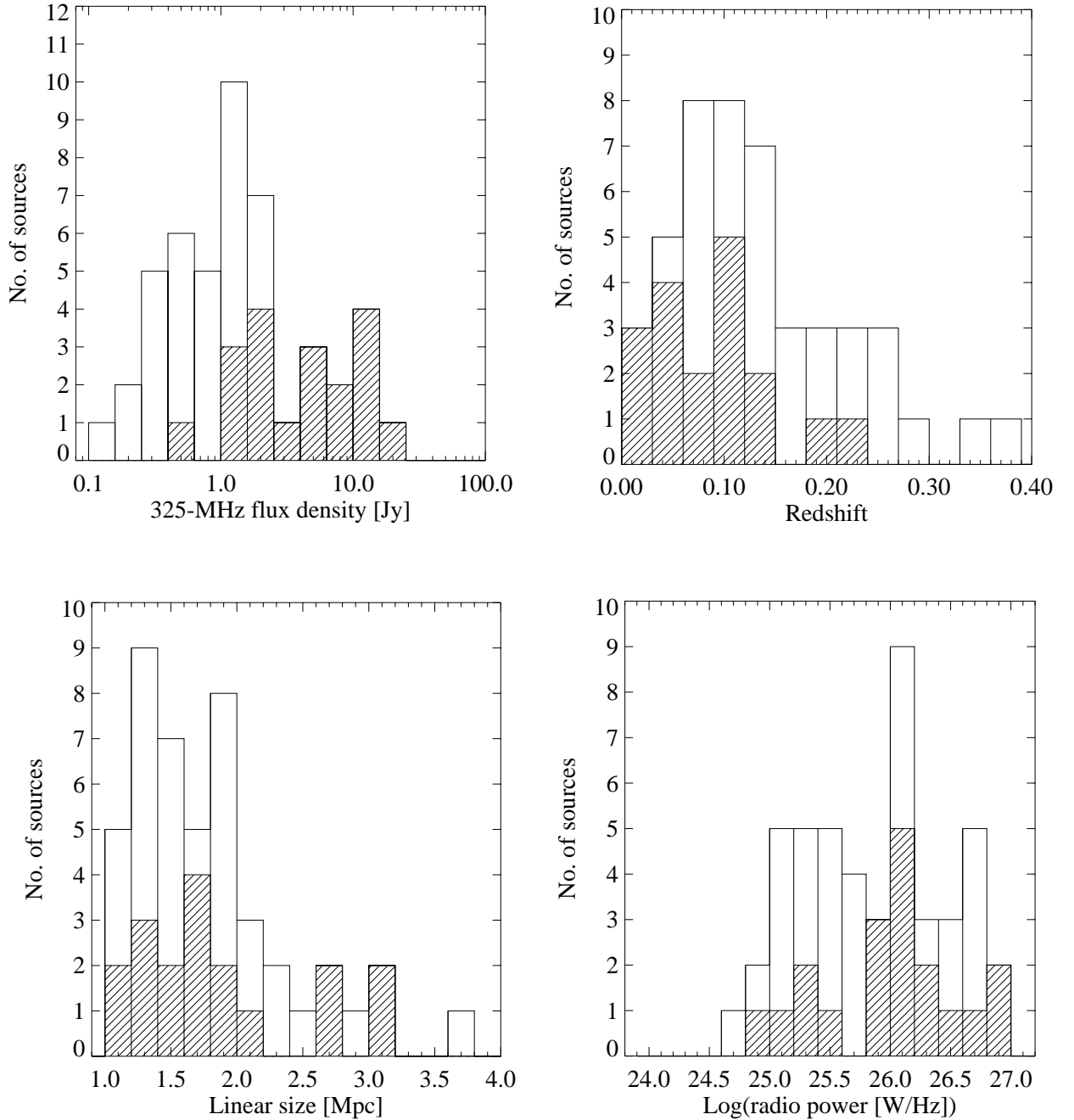


Fig. 1. Histograms of several properties of the new and old sample of GRGs. In all plots, the hatched bars indicate the distribution of previously known GRGs (see Table 1). **a)** (upper left): The 325-MHz flux density distribution of the GRGs. We have used a binsize of 0.2 in the logarithm of the flux density in Jy. **b)** (upper right): The redshift distribution of the GRGs, using a binsize of 0.03 in redshift. The source 8C 0821+695 at $z = 0.538$ lies outside the range of this plot. **c)** (lower left): The projected linear size distribution of the GRGs, using a binsize of 0.2 Mpc. The source 3C 236 ($D = 5.7$ Mpc) lies outside the range of this plot. **d)** (lower right): The rest-frame 325-MHz radio power distribution of the GRGs, using bins of width 0.2 in the logarithm of the radio power in WHz^{-1} .

(Fanaroff & Riley 1974) lies near 10^{26} WHz^{-1} , which is close to the median value of the combined sample (see Table 2).

5. Discussion

5.1. The “sensitivity limit” of WENSS

For a radio source to be included in our sample, it must be larger than $5'$ and it must have been noticed on the radio

maps as a large radio source. The latter is related to a surface brightness criterion: the average surface brightness, or integrated signal-to-noise ratio, must be high enough to be detected as a single radio source structure. The integrated signal-to-noise ratio, $(S/N)_{\text{int}}$, for a resolved radio source is given by

$$\left(\frac{S}{N}\right)_{\text{int}} \approx \frac{S_{\text{int}}}{\sigma\sqrt{A}}, \quad (1)$$

Table 2. Median values of some of the properties of the GRGs in the sample of “old” GRGs, the sample of new GRGs and the combined sample of 47 sources. Column 1 gives the property; Cols. 2 to 4 give the median value of these properties for the old, new and combined sample, respectively.

(1)	(2)	(3)	(4)
Property	Median values		
	Old	New	Comb.
S_{325} [Jy]	4.160	0.685	1.150
$\log(P_{325}$ [W Hz $^{-1}$])	26.041	25.625	25.951
Size [Mpc]	1.65	1.63	1.64
Redshift	0.099	0.1404	0.1175

where S_{int} is the integrated flux density of the source and the surface area A is in units of beams. The surface area can be rewritten as $A = c \cdot \theta_{\text{max}}^2$, where θ_{max} is the angular size (major axis) of the radio source and c is a number that relates the angular size to the surface area (cf. the length-to-width ratio). For instance, for an elliptically shaped radio source with a length-to-width ratio of 3, $c = \frac{\pi}{(12 \ln 2)} \cdot \theta_{\text{beam}}^2$ with θ_{beam} the ($FWHM$) beam-size of the observation. If we substitute the above expression for A in Eq. (1) we find

$$\left(\frac{S}{N}\right)_{\text{int}} \propto \frac{S_{\text{int}}}{\theta_{\text{max}}} \quad (2)$$

Figure 2 shows $S_{\text{int}}/\theta_{\text{max}}$ against θ_{max} for the sources in our sample which we have identified as GRGs. We find that the lowest values of $S_{\text{int}}/\theta_{\text{max}}$ for selected sources lie in the range between 0.02–0.03 Jy/arcmin; the source which lies well below this line is B 1044+745, which is one of the two sources that were selected only for its radio structure in the NVSS and should therefore be situated below the WENSS “sensitivity” limit. The other source which lies just below the line is B 1245+676, which was selected from the WENSS but can be considered a “border-line” case. The two sources just above the limit are B 0935+743 and B 1306+621.

The sensitivity limit appears to be almost independent of angular size at least up to a size of ~ 40 arcmin. The sensitivity of WENSS to objects with an angular size above 1 degree on the sky decreases, so that the sensitivity limit inevitably must rise eventually.

From the figure we conclude that sources with $\theta_{\text{max}} \geq 5'$ will most likely be selected if $S_{\text{int}}/\theta_{\text{max}} \gtrsim 0.025$ Jy/arcmin. We will use this criterium to specify the regions in the radio power – linear size – redshift (P, D, z) parameter space which is accessible by our selection.

5.2. The radio power – linear size diagram

In Fig. 3 we have plotted for all identified GRGs in our sample the linear size, D , against the radio power at 325 MHz, P , the so-called P – D diagram. For reference, all sources of the LRL sample with $z < 0.6$, which is the

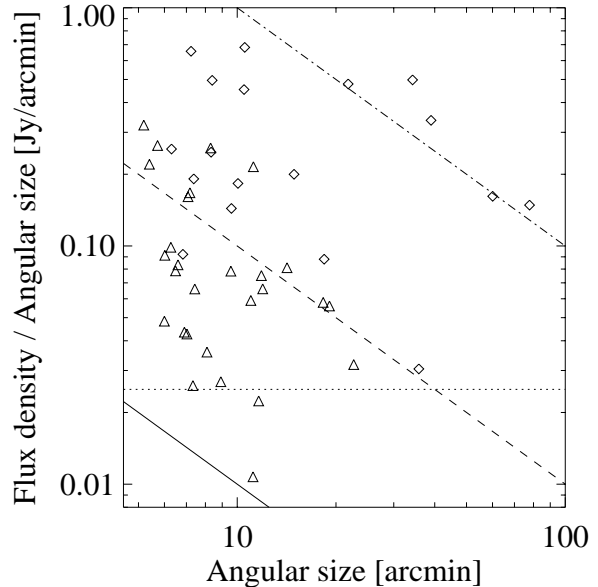


Fig. 2. A plot of the 325-MHz flux density divided by the angular size against the angular size for the “old” (diamonds) and the newly discovered GRGs (triangles). The diagonal lines indicate a constant integrated flux density and are drawn for 0.1 (solid), 1 (dashed) and 10 (dot-dashed) Jy. From this plot we determine the sensitivity limit of our selection method, ($S_{\text{int}}/\theta_{\text{max}} = 0.025$ Jy/arcmin), indicated by the dotted horizontal line.

same redshift range as in which the GRGs are found, are plotted as well. Note that several of the formerly known GRGs are part of the LRL sample; these have been plotted as LRL sources.

From this plot the following can be concluded. First, although we have conducted the most extensive systematic search for GRGs to date, there are no sources in the upper right part of the P – D diagram, i.e. the region occupied by sources with large size and high radio power. If such sources had existed in our search area, they would most likely have been discovered because of their inevitable high flux density. Second, the few GRGs which have a linear size above 2 Mpc have, on average, a higher radio power than smaller-sized GRGs.

To investigate which region of the P – D diagram is accessible through our WENSS selection, we have plotted in Fig. 4 lines which represent the lower sensitivity limit at constant redshift. Since the sensitivity limit is set by $S_{\text{int}}/\theta_{\text{max}} = 0.025$ Jy/arcmin (see Sect. 5.1), and a given redshift $S_{\text{int}} \propto P$ and $\theta_{\text{max}} \propto D$, the limit at that redshift follows the relation $P \propto D$. In Fig. 4 we have assumed a radio source spectral index of -0.8 to convert flux density into radio power.

At a particular redshift, WENSS can only detect giant sources which are more powerful than the radio power at which the line has been drawn (i.e. only in that part of the P – D diagram which is situated above the line). Note that lines of higher redshifts also start at a larger linear size because of the $5'$ lower angular size limit we have imposed. Based on the accessible regions in the P – D

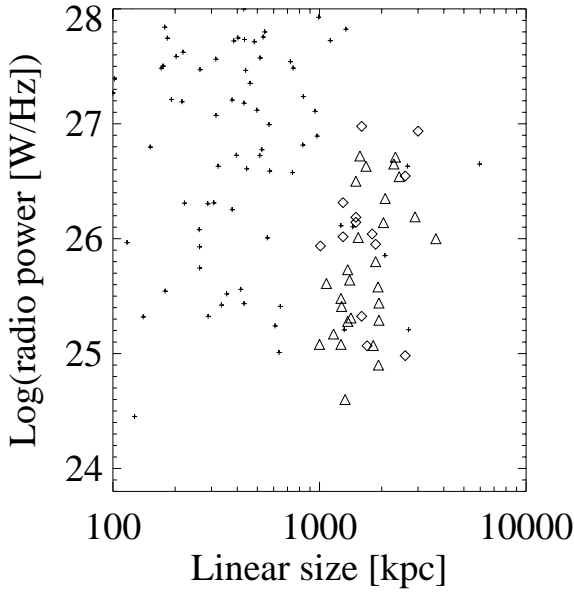


Fig. 3. The 325-MHz radio power against linear size P – D diagram for the formerly known GRGs not part of the LRL sample (diamonds), the newly discovered GRGs (triangles) and sources from the LRL sample with $z < 0.6$ (plusses).

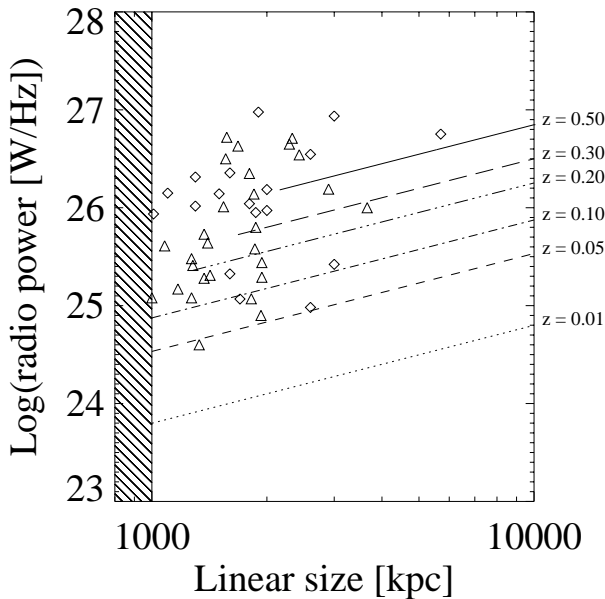


Fig. 4. P – D diagram, filled with formerly known GRGs (diamonds) and newly discovered GRGs (triangles). The lines indicate the lower radio power limit for a source at a particular redshift as a function of linear size; the area directly above such a line is the accessible region in the (P, D) parameter space at that redshift. See text for further details.

diagram there is no apparent reason why sources larger than 2 Mpc should be missed.

5.3. Radio power and linear size versus redshift

In Fig. 5a we have plotted the 325-MHz radio powers of the GRGs against their redshifts. The higher sensitivity of the WENSS, as compared to earlier surveys, has enabled

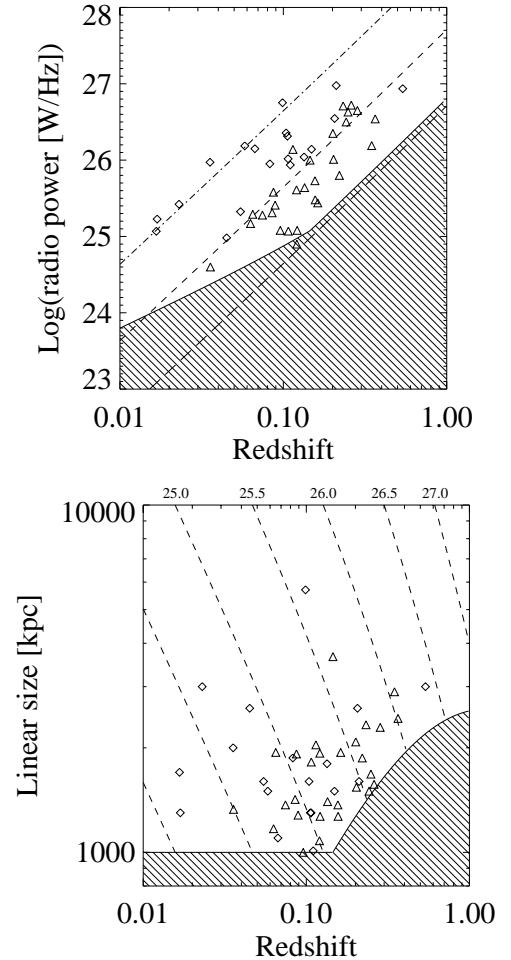


Fig. 5. **a)** (Top) The 325-MHz radio power against the redshift of the formerly known (diamonds) and newly discovered (triangles) GRGs. The three diagonal lines represent the radio power for sources with a 325-MHz flux density of 0.1 Jy (long-dashed), 1.0 Jy (dashed) and 10.0 Jy (dot-dashed), assuming a spectral index of -0.8 . The hatched area indicates the part of the diagram in which sources fall below our sensitivity limit. **b)** (Bottom) The projected linear sizes of the GRGs against their redshift. The meaning of the symbols is the same as in the upper plot. The hatched area indicates the region of the plot in which sources have not been selected, either because they are physically smaller than 1 Mpc, or spatially smaller than $5'$. The dashed lines indicate the sensitivity limit for sources of the particular radio power is indicated (in logarithmic units of W Hz^{-1} at 325 MHz) on top of each line. We assume a spectral index of -0.8 . Sources can only be detected if they lie to the left of the line belonging to their particular radio power.

the discovery of GRGs with 5–10 times lower radio power. The hatched region in the figure indicates the part of the parameter space which is not accessible by WENSS, as a result of its limited sensitivity and lower angular size limit. Again, in determining this region we have assumed a spectral index of -0.8 for the radio sources, but the upper edge of the region is not very sensitive to the spectral index.

The broken shape of the upper edge of the hatched region can be understood as follows. At all redshifts, the

WENSS is most sensitive to physically, and thus spatially, small sources. Since both a lower angular and physical size limit have been imposed, there are two regimes in which each of these two limits is in effect. At very low redshifts, a source with a physical size of 1 Mpc extends over $5'$ on the sky. This leads to a surface brightness limit and the integrated flux density of the source thus has to be large for the source to be still detectable. At higher redshift, the selection is constrained by the $5'$ lower angular size limit. This results in a lower limit to the flux density of a detectable source, determined by $S_{\text{int}} \geq 0.025 [\text{Jy/arcmin}] \cdot 5 [\text{arcmin}] = 0.125 \text{ Jy}$. Thus, we are flux density limited. The break occurs at that redshift at which a 1-Mpc large radio source will span an angle of $5'$ on the sky ($z \sim 0.146$).

The one source that just lies in the hatched area where no sources should have been found is B 1044+745, which, as mentioned before, would indeed not have been selected on basis of the WENSS data.

The strong effect that the lower angular size limit has on the selection can best be seen in Fig. 5b, where we have plotted the projected linear size of the identified GRGs against their redshift. Again, the hatched area indicates the region of the diagram which is inaccessible. The strong “bump” at redshifts above ~ 0.15 result from the lower angular size limit.

Furthermore, in Fig. 5b we have plotted the sensitivity limit for sources of constant radio power (dashed lines). The (logarithm of the) radio power (in WHz^{-1} at 325 MHz) for each particular line has been indicated at the top of the diagram. A radio source of radio power P and linear size D can only be selected if it has redshift below that indicated by the dashed line for power P at size D . Had that source been at a higher redshift, or had it been of larger linear size, it would not have been selected. Likewise, all sources which lie on the left of such a line of constant P , should all have a radio power below this value. Apart from the before-mentioned case of B 1044+745, this is indeed the case for the identified GRGs in our sample.

5.4. The 2-Mpc linear size cut-off

A strong drop in the number of sources with projected linear size above 2 Mpc has been found (see Fig. 1c). This may be a result of a strong negative radio power evolution of radio sources with increasing size, combined with our sensitivity limit. A negative radio power evolution is indeed expected for active radio radio sources (cf. Kaiser et al. 1997; Blundell et al. 1999). On the other hand, the observed effect can also be caused if a substantial fraction of the GRGs stop their radio activity (and “fade”) before they reach a size of 3 Mpc.

Above, we have argued that the selection effects alone provide no apparent reason why sources of linear size above 2 Mpc should have been missed if they existed in large numbers. On the contrary, Fig. 5b shows that sources above 2 Mpc in size can potentially be selected out to

much higher redshift than smaller sized sources. Indeed, the figure shows that the majority of identified 2–3 Mpc large sources have redshifts at which 1-Mpc large sources would not have been selected.

Therefore, the observed 2-Mpc cut-off must be caused by a combination of the internal luminosity evolution of the sources and the sensitivity of the WENSS. An extreme case of such a luminosity evolution occurs when a large fraction of giant sources do not remain active for a long enough amount of time to reach a linear size of 2 Mpc. To disentangle the effects of the luminosity evolution of active and so-called “relic” sources on the observed number of sources as a function of linear size requires much better statistics on the death-rate of radio galaxies as a function of radio power and linear size.

Acknowledgements. The INT and WHT are operated on the island of La Palma by the Isaac Newton Group in the Spanish Observatorio del Roque de los Muchachos of the Instituto de Astrofísica de Canarias. The Westerbork Synthesis Radio Telescope (WSRT) is operated by the Netherlands Foundation for Research in Astronomy (NFRA) with financial support of the Netherlands Organization for Scientific Research (NWO). The National Radio Astronomy Observatory (NRAO) is operated by Associated Universities, Inc., and is a facility of the National Science Foundation (NSF). This research has made use of the NASA/IPAC Extragalactic Database (NED) which is operated by the Jet Propulsion Laboratory, California Institute of Technology, under contract with the National Aeronautics and Space Administration. The Digitized Sky Surveys were produced at the Space Telescope Science Institute under U.S. Government grant NAG W-2166. The images of these surveys are based on photographic data obtained using the Oschin Schmidt Telescope on Palomar Mountain and the UK Schmidt Telescope. The plates were processed into the present compressed digital form with the permission of these institutions. M. N. Bremer, H. Sangheera and D. Dallacasa are thanked for their help in the early stages of this project. P. Best and M. Lehnert are thanked for many helpful discussions and suggestions. L. Lara is acknowledged for providing high resolution radio maps of several sources prior to publication.

References

- Barthel, P. D. 1989, ApJ, 336, 606
- Becker, R., White, R., & Helfand, D. 1995, ApJ, 450, 559
- Bhatnagar, S., Gopal-Krishna, & Wisotzki, L. 1998, MNRAS, 299, L25
- Blundell, K., Rawlings, S., & Willott, C. J. 1999, AJ, 117, 677
- Burbidge, E. M., & Strittmattar, P. A. 1972, ApJ, 172, L37
- van Breugel, W. J. M., & Willis, A. G. 1981, A&A, 96, 332
- van Breugel, W. J. M., & Jägers, W. 1982, A&AS, 49, 529
- de Bruyn, A. G. 1989, A&A, 226, L13
- Colla, G., Fanti, C., Fanti, R., et al. 1975, A&AS, 20, 1
- Condon, J. J., Cotton, W. D., Greisen, E. W., et al. 1998, AJ, 115, 1693
- Demoulin, M. 1970, ApJ, 160, L79
- Dingley, S. J. 1990, Ph.D. Thesis, University of Cambridge
- Djorgovski, S. G., Thompson, D., Vigotti, M., & Grueff, G. 1990, PASP, 102, 113
- Djorgovski, S. G., Thompson, D., Maxfield, L., Vigotti, M., & Grueff, G. 1995, ApJS, 101, 255

- Falle, S. A. E. G. 1991, MNRAS, 250, 581
Fanaroff, B. L., & Riley, J. M. 1974, MNRAS, 167, 31
Faulkner, M. A. 1985, Ph.D. Thesis, Univ. of Cambridge
Fomalont, E. B., & Bridle, A. H. 1978, AJ, 83, 7
de Grijp, M. H. K., Keel, W. C., Miley, G. K., Goudfrooij, P., & Lub, J. 1992, A&AS, 96, 389
Hine, R. G. 1979, MNRAS, 189, 527
Ishwara-Chandra, C. H., & Saikia, D. J. 1999, MNRAS, 309, 100
Jägers, W. J. 1986, Ph.D. Thesis, University of Leiden
Kaiser, C. R., & Alexander, P. 1999, MNRAS, 302, 515
Kaiser, C. R., Dennett-Thorpe, J., & Alexander, P. 1997, MNRAS, 292, 723
Lacy, M., Rawlings, S., Saunders, R., & Warner, P. J. 1993, MNRAS, 264, 721
Laing, R. A., Riley, J. M., & Longair, M. S. 1983, MNRAS, 204, 151
Lara, L., Cotton, W. D., Feretti, L., et al. 2001, A&A, in press
Mack, K.-H., Klein, U., O'Dea, C. P., & Willis, A. G. 1997, A&AS, 123, 423
Mack, K.-H., Klein, U., O'Dea, C. P., Willis, A. G., & Saripalli, L. 1998, A&A, 329, 431
Marcha, M. J. M., Browne, I. W. A., Impey, C. D., & Smith, P. S. 1996, MNRAS, 281, 425
Masson, C. R. 1979, MNRAS, 187, 253
Miley, G. K., & Osterbrock, D. E. 1979, PASP, 92, 257
Palma, C., Bauer, F. E., Cotton, et al. 2000, AJ, 119, 2068
Parma, P., de Ruiter, H. R., Mack, K.-H., et al. 1996, A&A, 306, 708
Parma, P., Murgia, M., Morganti, R., et al. 1999, A&A, 344, 7
Perley, R. A., Bridle, A. H., & Willis, A. G. 1984, ApJS, 54, 291
Rengelink, R., Tang, Y., de Bruyn, A. G., et al. 1997, A&AS, 124, 259
Riley, J. M. 1989, MNRAS, 238, 1055
Riley, J. M., Warner, P. J., Rawlings, S., et al. 1988, MNRAS, 236, 13
Röttgering, H. J. A., Tang, Y., Bremer, M. A. R., et al. 1996, MNRAS, 282, 1033
Sargent, W. L. W. 1973, ApJ, 182, L13
Saunders, R. D. E. 1982, Ph.D. Thesis, University of Cambridge
Saunders, R. D. E., Baldwin, J. E., & Warner, P. J. 1987, MNRAS, 225, 713
Saripalli, L., Gopal-Krishna, Reich, W., & Kühr, H. 1986, A&A, 170, 20
Scheuer, P. A. G. 1974, MNRAS, 166, 513
Schoenmakers, A. P. 1999, Ph.D. Thesis, Utrecht University
Schoenmakers, A. P., de Bruyn, A. G., Röttgering, H. J. A., & van der Laan, H. 1999, A&A, 341, 44
Schoenmakers, A. P., de Bruyn, A. G., Röttgering, H. J. A., van der Laan, H., & Kaiser, C. R. 2000a, MNRAS, 315, 371
Schoenmakers, A. P., Mack, K.-H., de Bruyn, A. G., et al. 2000b, A&AS, 146, 293
Simien, F., & Prugniel, P. 1997, A&AS, 122, 521
Spinrad, H., Djorgovski, S., Marr, J., & Aguilar, L. 1985, PASP, 97, 932
Strom, R. G., & Willis, A. G. 1980, A&A, 85, 36
Strom, R. G., Baker J. R., & Willis, A. G. 1981, A&A, 100, 220
Strom, R. G., Fanti, R., Parma, P., & Ekers, R. D. 1983, A&A, 122, 305
Subrahmanyam, R., & Saripalli, L. 1993, MNRAS, 260, 908
Vigotti, M., Grueff, G., Perley, R., Clark, B. G., & Bridle, A. H. 1989, AJ, 98, 419
Wagett, P. C., Warner, P. J., & Baldwin, J. E. 1977, MNRAS, 181, 465
Wieringa, M. 1991, Ph.D. Thesis, University of Leiden
Willis, A. G., Strom, R. G., & Wilson, A. S. 1974, Nature, 260, 625
Willis, A. G., Strom, R. G., Bridle, A. H., & Fomalont, E. B. 1981, A&A, 95, 250